Performance Analysis of PSO-Based SHEPWM Control of Clone Output Nine-Switch Inverter for Nonlinear Loads

Nirmala Muthusamy[1,*], Beena Stanislaus Arputharaj[2], Vijayanandh Raja[3]
[1]*Department of Electrical and Electronics Engineering, Kumaraguru College of Technology,
Coimbatore-641049, Tamil Nadu, India*
[2]*Department of Research and Innovation, Saveetha School of Engineering, SIMATS,
Chennai-602105, Tamil Nadu, India*
[3]*Department of Aeronautical Engineering, Kumaraguru College of Technology,
Coimbatore-641049, Tamil Nadu, India*
nirmala.m.eee@kct.ac.in; beena2192@gmail.com; vijayanandh.raja@gmail.com

Abstract—A comprehensive mathematical model of the inverter using nine switches is derived and its carrier high-frequency signal-based Pulse Width Modulation (PWM) is developed for the control of dual nonlinear loads. The Carrier-Based Pulse Width Modulation (CBPWM) provides excellent quality output to linear loads, and it provides high value of Total Harmonic Distortion (THD) for the nonlinear load, where the 5th, 7th, 11th, 13th, and 17th harmonics are highly manifest. Particle Swarm Optimisation (PSO) constructed Selective Harmonic Elimination Pulse Width Modulation (SHEPWM) scheme is proposed to eliminate a higher number of harmonic components and enhance the harmonic profile with reduced number of active semiconductor switches in Nine-Switch Inverter (NSI) control of nonlinear load. The PSO algorithm is proposed to adjust the triggering angles of the SHEPWM scheme and eliminate the targeted harmonics. The main concern associated with the proposed technique is the degree of freedom to lower the harmonics when operated over a comprehensive scale of Modulation Index (MI). To prove the usefulness of the proposed carrier-based PWM, PSO-based SHEPWM technique for NSI, MATLAB-SIMULINK is used to perform the simulations. The experimental prototype of the NSI topology is developed using an ATmega162 microcontroller. The experimental results and its Fast Fourier Transform (FFT) spectrum are over a broad scale of MI, revealing the expertise and efficacy of the proposed control scheme.

Index Terms—Particle Swarm Optimisation (PSO); Fast Fourier Transform (FFT) spectrum; Selective Harmonic Elimination Pulse Width Modulation (SHEPWM); Carrier-Based Pulse Width Modulation (CBPWM); Total Harmonic Distortion (THD); Modulation Index (MI).

I. Introduction

Currently, inverters are widely employed to regulate the voltage and frequency of alternating-current loads. The power electronics sector encounters numerous obstacles in the advancement of Electric Vehicles (EVs) and Hybrid Electric Vehicles (HEVs). The nine-switch converter is a new topology used for the autonomous management of dual AC loads and in unified power quality conditioners. Applications such as vehicle propulsion systems, hybrid electric vehicles, rotary wing aircraft, and robotics require the usage of two or more motors and require autonomous control [1]. There are two potential control methods. The first way involves controlling each motor using two inverters. The second method involves using a single inverter to drive two motors that are connected in parallel. The drawback of the former method is that it increases the expense of the experimental equipment, whereas the latter method allows for dependent control of the dual motors [2]. Consequently, the suggested nine-switch inverter can control dual independent loads in a distinct manner. The primary objective in designing a power electronic circuit is to minimise the utilisation of both active and passive components. The benefits of a nine-switch inverter include a reduced occurrence rate, ease of control, and high reliability resulting from the fewer number of power electronic components required for the triggering circuit. The nine-switch converter consists of two inverters, each equipped with three shared switches [3].

The nine-switch converter is equipped with two distinct outputs: an upper output and a lower output. The first segment of the converter that includes the upper and middle switches (T1U, T4U, T7U and T2M, T5M, T8M) is called as NSI_1. The second converter consists of the middle and lower switches (T2M, T5M, T8M and T3L, T6L, T9L) and is called NSI_2. The DC connection voltage in the two sets of classical two-level six-switch voltage source converters requires a higher voltage rating. The centre switches in the schematic arrangement depicted in Fig. 1 are utilised by both NSI_1 and NSI_2, two sets of output that are interdependent and limit independent control over magnitude and frequency [4].

The modulating signals of NSI_1 vital should always be larger than the modulating signals of NSI_2. This is accomplished by adding a suitable random selection of DC offset voltage to both modulating signals. The Converter 1 reference is increased by 25 % of the DC voltage, while the Converter 2 reference is decreased by the same amount. This adjustment compensates for the DC offset voltage, which is equal to the difference between the highest and lowest phase

voltages for the Converter 1 and Converter 2 references, respectively [5]–[7].
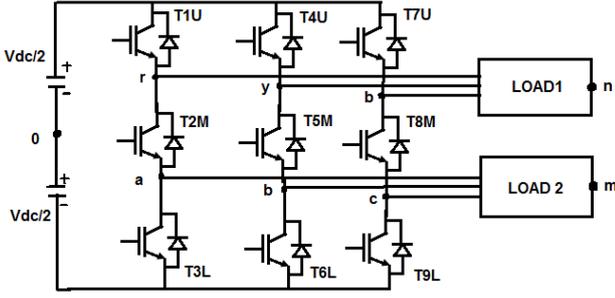
Fig. 1. Control of nine-switch converter of two independent loads [2].

II. CONTROL OF NINE-SWITCH INVERTER

With the intention of preventing the DC source from shortening, it is necessary to adhere to Kirchhoff's current and voltage laws and ensure the continuity of current flow. Therefore, it is necessary to satisfy the constraint specified in (1) regarding the switching utility in order to achieve this requirement

$$ST_{iU} + ST_{iM} + ST_{iL} = 2. \tag{1}$$

The upper, middle, and lower leg switches have switching functionalities denoted ST_{iU}, ST_{iM}, and ST_{iL}, respectively. When the switches are activated, ST is set to one, and when the switches are deactivated, ST is set to zero. The subscripts i = a, b, c refer to the phase output associated with the switch. U, M, and L indicate the devices of the upper, middle, and lowest legs of the converter, respectively. The dual output nine-switch converters can be controlled using either a Common Frequency (CF) control mode or a Different Frequency (DF) control mode. These control modes are used for two different linear loads. To generate the upper and lower outputs of nine-switch inverter (NSI) using the CBPWM technique, two distinct reference signals are combined with a carrier signal that is high frequency. This combination results in gating signals for NSI$_1$ and NSI$_2$. The magnitude, switching frequency, and phase of the two reference signals are denoted as V_1, f_1, φ_1 and V_2, f_2, φ_2, respectively. Table I provides a comprehensive overview of the active switching states during the R phase. The EXOR values of the two comparator outputs are used to trigger the three middle switches. The R-phase reference signals for NSI$_1$ and NSI$_2$ are denoted V_{R1}^{ref} and V_{R2}^{ref}, respectively. These signals are calculated by (2) and (3):

$$V_{R1}^{ref} = V_1 + \sin(2\Pi f_1 t + \varphi_1), \tag{2}$$

$$V_{R2}^{ref} = V_2 + \sin(2\Pi f_2 t + \varphi_2). \tag{3}$$

The modulation index is calculated using (4)

$$m = \frac{V^{ref}}{V_{dc}/2}. \tag{4}$$

There are a total of 12 possible active switching states. Table I provides a list of three states for each phase that can be easily identified.

TABLE I. SWITCHING STATE FOR THE R PHASE FOR NSI.

State	ST1U	ST2M	ST3L	V$_{jo}$	V$_{ko}$
1	0	1	1	0.5 Vdc	0.5 Vdc
2	1	0	1	0.5 Vdc	-0.5 Vdc
3	1	1	0	-0.5 Vdc	-0.5 Vdc

In Table I, V_{j0} and V_{k0} are the phase R to the midpoint of the DC link voltages, j = r, y, b; k = x, y, z. V_{dc} is the voltage of the DC link. The switching functions of the top and bottom devices are expressed in (5) and (6) as follows:

$$ST_{iU} = (V_{n0} + V_{jn})/V_{dc} + 0,5, \tag{5}$$

$$ST_{iL} = -(V_{m0} + V_{km})/V_{dc} + 0.5. \tag{6}$$

Evaluation of the reference signal with the triangular carrier high-frequency signal allows the generation of triggering pulses for nine-switch inverters. The nine-switch converter has a dual output, which allows for the comparison of two modulation signals that indicate the upper and lower switches with a single triangle carrier signal. Equations (7) and (8) provide the fundamental principle that governs the generation of the triggering pulses to fulfil the twin concepts of satisfying the triggering function restriction:

$$St_{iU} = \begin{cases} 1, M_{iU} \geq V_{triangle}, \\ 0, everywhere\ else, \end{cases} \tag{7}$$

$$ST_{iL} = \begin{cases} 1, M_{iL} \leq V_{triangle}, \\ 0, everywhere\ else. \end{cases} \tag{8}$$

The modulation signals for the top and lower switches are denoted as Mi_U and Mi_L, respectively, while the high-frequency triangular signal is represented as $V_{triangle}$. The magnitude of the output voltage, Mi_U, is consistently higher than the magnitude of the input voltage, Mi_L, due to injection of zero sequence voltage into the reference signals. The top switching device switching functions are derived from (9)

$$ST_{iU} = 2 - ST_{iM} - ST_{iL}. \tag{9}$$
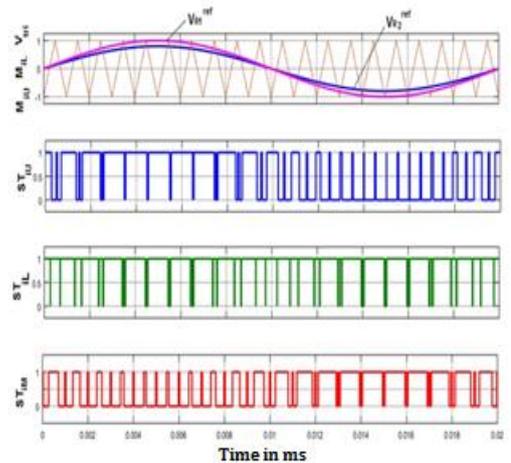
Fig. 2. Generation of gating pulse for switching devices.

The control of generating gating pulses for switching devices in an NSI is demonstrated in Fig. 2 using carrier-based pulse width modulation (CBPWM). Each segment is equipped with both upper and lower reference signals. The

top and inferior outputs of the NSI are linked to these reference signals.

The carrier signal is compared with the equivalent phase upper reference signal (VR$_1$^{ref}) to generate the upper switch trigger signal. In the same manner, the lower reference signal and the carrier signal of the corresponding phase (VR$_2$^{ref}) are compared to generate the lower switch-triggering signal. The centre switch triggering signal is produced by performing a logical EXOR operation on the upper and lower triggering signals of switches, as depicted in Fig. 3. This strategy ensures that two switches in each inverter leg are consistently turned on.
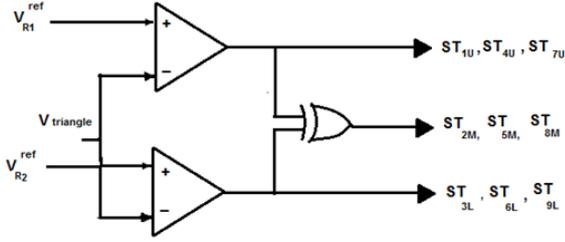
Fig. 3. Triggering pulse generation for middle switches using the XOR gate [4].

Dead periods are automatically inserted during the EXOR process to protect the converter from accidental short circuits. This is done by incorporating appropriate dead times into the NSI, which helps regulate a normal VSI. NSI has a total of 12 switching states, consisting of nine active states and three zero states. Each phase leg has only three valid switching states, consisting of four vectors that do not involve zero and two zero vectors (000,111) for both outputs. Each switching cycle consists of six vectors. However, while one output has a vector consisting of all zeros (000), the second output contains a vector consisting of all ones (111). The NSI can be operated in Constant Frequency mode (CF Mode) or Variable Frequency mode (VF Mode) [8]–[11].

III. SHEPWM-Based Control of NSI Fed Nonlinear Loads

The principles of the harmonic elimination technique involve the analytical elimination of any desired number of harmonics. This can be achieved utilising a generalised method specifically designed for the dual output nine-switch inverter. The primary square wave is divided several times based on a consistent relationship between the number of divisions and the expected number of eliminated harmonics [12]. Figure 4 illustrates the N divisions per half-cycle of the overall output waveform. The periodic waveform is considered to have half-wave symmetry, as described in (10) and having unit amplitude

$$f(\omega t) = -f(\omega t + \pi),\qquad(10)$$

where f(ωt) is a dual-state cyclic function with N chops per half-cycle. Let α_1, α_2, α_3, ..., α_{2M} define the N chops.

A Fourier series expression is represented in (11)

$$f(\omega t) = \sum_{n=1}^{\infty}(a_n \sin(n\omega t) + b_n \cos(n\omega t)),\qquad(11)$$

where:

$$a_n = \frac{1}{\pi}\int_0^{2\pi} f(\omega t)\sin(n\omega t)d\omega t,\qquad(12)$$

$$b_n = \frac{1}{\pi}\int_0^{2\pi} f(\omega t)\cos(n\omega t)d\omega t.\qquad(13)$$
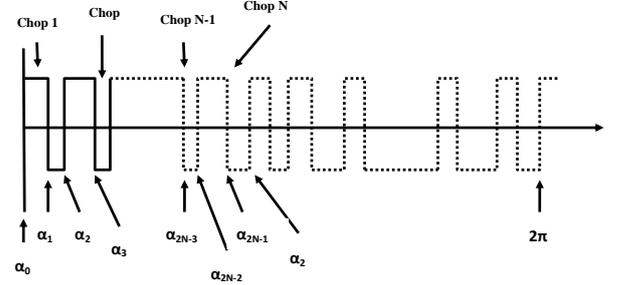
Fig. 4. Normalised magnitude output waveform of the voltage source inverter [4].

In (14), substitute for $f(\omega t)$, and using the half-wave symmetry property,

$$a_n = \frac{2}{\pi}\sum_{k=0}^{2N}(-1)^k \int_{\alpha_K}^{\alpha_{K+1}} sin(n\omega t)d\omega t.\qquad(14)$$

From (14), evaluating the integral,

$$\left|\begin{array}{l} a_n = \frac{2}{n\pi}\sum_{k=0}^{2N}(-1)^K\left[cos(n\alpha_K)-cos(n\alpha_{K+1})\right] \\ a_n = \frac{2}{n\pi}\left[cos\, n\,\alpha_o - cos\, n\,\alpha_{2N+1} + 2\sum_{K=1}^{N}(-1)^K cos\, n\,\alpha\right] \end{array}\right|.\qquad(15)$$

The known boundary conditions are: $cos\, n\alpha_o = 1$; $cos\, n\alpha_{2N+1} = (-1)^n$. Henceforth, (15) reduces to

$$a_n = \frac{2}{n\pi}\left|1-(-1)^K + 2\sum_{k=1}^{2N}(-1)^K cos\, n\alpha_k\right|.\qquad(16)$$

By exploiting the half-wave symmetry property of the waveform, it can be determined that a_n and b_n are both equal to zero for even values. Thus, for odd values of n, (15) and (16) depend on 2N variables:

$$b_n = -\frac{4}{n\pi}\left|\sum_{k=1}^{2N}(-1)^k \sin n\alpha_K\right|,\qquad(17)$$

$$a_n = -\frac{4}{n\pi}\left|1+\sum_{k=1}^{2N}(-1)^k \cos n\alpha_K\right|.\qquad(18)$$

To obtain a unique solution for the 2N variables, it is necessary to have 2N equations. These equations can be constructed from (17) and (18) by setting any N harmonics equal to zero. An algebraic method is used to eliminate harmonics. One of the primary challenges in power electronic circuits is determining the precise timing of the gate pulse to switch the power electronic devices. Mathematical analysis is employed to resolve the nonlinear simultaneous harmonic equations. The nonlinear equations are transcendental

equations and solved by proper transformations to achieve the final optimum angles employed in the creation of PWM pulses for the intended harmonics elimination. The switching angles are obtained by obtaining the solutions of the provided set of harmonic equations by utilising nonlinear iterative approach. The generalised harmonic equation of power electronic inverters is provided by the expression (19)

$$V_{2k+1} = \frac{4V_{dc}}{(2k+1)\pi} \sum_{i=0}^{N} h_i \cos(2k+1)\alpha_i, \quad (19)$$

where V represents the inverter voltage output, Vdc represents the input direct current (DC) voltage, h_i represents the fluctuation of waveform level, α represents the angle of triggering of the inverter, N represents the number of harmonic equations, and K represents the number of switching angles, which ranges from 0 to N-1. The quantity of harmonics reduced depends upon the number of switching angles that may be optimised. The mathematical expression

of Selective Harmonic Elimination Pulse Width Modulation (SHEPWM) entails solving a set of nonlinear equations simultaneously. The equations in question possess several local minima, making the process of finding the precise solution intricate [13]. The SHEPWM approach offers the advantage of eliminating lower-order harmonics (LOH), leading to reduced filtering needs and lower costs. Additionally, performance indices such as total harmonic distortion (THD) can be tuned to address various power quality problems.

The objective function of SHEPWM is to eliminate the occurrence of three-fold harmonics when operating a balanced load with a three-phase inverter. To eliminate the lower-order 5th, 7th, 11th, 13th, 17th, and 19th odd harmonics from the output voltage of the inverter, the Particle Swarm Optimisation (PSO) technique is utilised. This is done by selecting a desired value for the fundamental quantity within. To find the solution, (20) should be used to minimise the THD by utilising the objective function stated in (20)

$$F_i = \min \left\{ \frac{16}{\pi^2} \left[\left(1 + \sum_{k=1}^{\infty} (-1)^k \cos(\alpha_k) - M \right) \right]^2 + \left[\left(1 + \sum_{k=1}^{\infty} (-1)^k \cos(n\alpha_k) \right) \frac{4}{n\pi} \right]^2 \right\}. \quad (20)$$

The following constraint is considered for the objective function F_i in (21)

$$0 < \alpha1 < \alpha2 < \alpha3 < \alpha4 < \alpha5 < \alpha6 < \alpha7 < \alpha8 < \alpha9 < 90. \quad (21)$$

Meta-heuristic algorithms are global search techniques that draw inspiration from biological evolution and often employ a population-based approach to iteratively improve solutions to a given problem [14]. Global search algorithms possess the benefit of being highly resilient, hence increasing the likelihood of discovering the ideal solution within a vast search field. To mitigate the presence of specific harmonics (namely the 5th, 7th, 11th, 13th, 17th, and 19th harmonics), we aim to utilise firing angles derived from PSO to control a three-phase nine-switch inverter.

The primary objective of implementing nonlinear load control in a nine-switch inverter is to remove explicit odd harmonics, such as the 5th, 7th, 11th, 13th, 17th, and 19th harmonics. To accomplish this, the pulse width of the switches is adjusted by generating different firing angles at which the switches are activated. The optimised firing angles are obtained by using PSO [15]. The purpose of this device is to eliminate harmonics from the output of the nine-switch inverter. Triggering angles are obtained throughout the viable range of the modulation index, which ranges from 0.1 to 1 [16]. This strategy has been shown to be efficient based on the acquired results by eliminating the undesired lower-order harmonics. PSO emulates the sociological behaviour characteristic of swarm intelligence, like the synchronised flight of a flock of birds. The PSO algorithm is mathematically represented by location and velocity vectors that determine the movement of the solution throughout the search space. Each member of the population is referred to as a particle, representing a potential solution to the problem. It explores the solution space by flying at a specific velocity to find the optimal spot. The location vector is represented as $X_i = [X_{i1}, X_{i2}, ..., X_{iN}]$, while the velocity vector is represented as $Vi = [V_{i1}, V_{i2}, ..., V_{iN}]$. Each individual particle inside the

swarm improves its hunting ability by considering its current velocity, experience, and the collective experience of nearby particles. The most optimal position of a particle achieved thus far is referred to as the local best (L_{best}), whereas the best position within the entire region of the swarm is known as the global best (G_{best}). The velocity of particle movement is regulated by an inertia weight (W). The particle regulates its velocity and position based on the determination of the two most optimal values. The velocity is recalculated using (22), and the individual position is updated using (23):

$$V_i^{(k+1)} = WV_i^{(k)} + c_1 r_i \left(L_{besti} - x_i^{(k)} \right) + c_2 r_2 \left(G_{besti} - x_i^{(k)} \right), \quad (22)$$

$$x_i^{(k+1)} = x_i^{(k)} + V_i^{(k+1)}, \quad (23)$$

where W is the weight factor of inertia, $V_i^{(k+1)}$ is the particle velocity in k^{th}_iteration, $x_i^{(k)}$ is the position of the particles in the search space in the kth iteration, c_1 and c_2 are the acceleration constants that are positive, and r_1 and r_2 are arbitrary numbers among (0, 1). i is the particle index, x_i is the position of the ith particle, and v_i is the velocity of the ith particle. The simulation parameters of the PSO algorithm are given in Table II.

TABLE II. PARAMETER CONSTRAINTS USED IN PSO ALGORITHM.

PSO Parameters Constraints	Values
Number of iterations (stopping criteria)	100
V_{in}, V_{max}	10, 20
Number of particles	10
Inertia weight W	0.95
c_1, c_2	1.5, 2.0
r_1, r_2	Random (0, 1)

IV. SIMULATION RESULTS

The discussion focusses on the simulation findings of Particle swarm optimisation (PSO)-based selective harmonic elimination pulse width modulation (SHEPWM) control of nine-switch inverter (NSI) for a nonlinear load. PSO

algorithm for SHEPWM control of NSI: The PSO method is utilised to solve the objective function. The algorithm is tested using the SHEPWM technique and the outcomes are evaluated according to the global minimum solution. Equation (20) is utilised as the objective function to solve the SHEPWM approach in F_i. The F_i fitness values are evaluated over 100 iterations using the PSO algorithm, and the convergence plot is depicted in Fig. 5.

The plot clearly demonstrates that the objective function achieved in all runs using the PSO method falls within the range of 0.01 to 0.03. By analysing the convergence plot, it can be observed that the THD reaches a small optimum zone of 3.96 %. Figure 6 shows the change in the switching angles with different modulation indices.
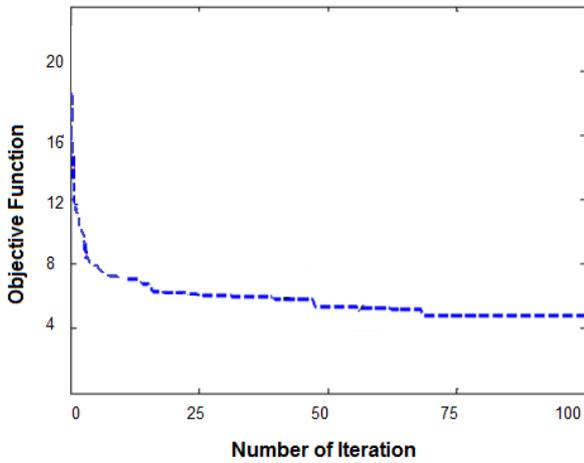
Fig. 5. Convergence plot for the PSO algorithm.
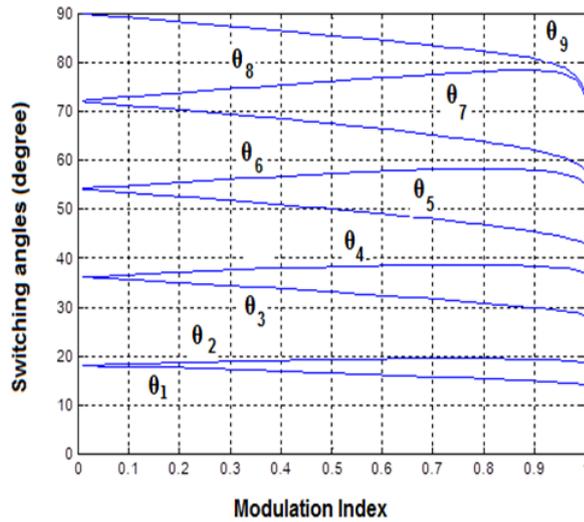
Fig. 6. Variation in PSO-based switching angles with various values of modulation index.

Table III shows the switching angles obtained using the PSO approach for various modulation index values ranging from 0.1 to 1 [17], [18]. Table IV provides the specific values for the individual selective odd harmonics (5th, 7th, 11th, 13th, 17th, and 19th) and the THD for various modulation index values ranging from 0.1 to 1. Table III demonstrates that the THD of the output voltage for a nine-switch inverter, when supplied to nonlinear loads, is 3.96 % when utilising the PSO-based selective harmonic elimination method with a Modulation Index (MI) of 1. This result is relatively low compared to the THD achieved with the carrier-based pulse

width modulation (CBPWM) control-based nine-switch inverter. The PSO algorithm is utilised to determine the switching angles for different modulation indexes. These angles are then used to calculate the amplitude of the Fourier coefficients for the lower-order harmonics that are of importance. This configuration can be achieved by analysing the results of equations and employing the approach of calculating switching angles.

TABLE III. SWITCHING ANGLES FOR VARIOUS MODULATION INDEX.

Switching Angles (α_1-α_5)				
MI	**α_1**	**α_2**	**α_3**	**α_4**	**α_5**
0.1	18.29	18.39	35.4	36.5	53.2
0.2	17.47	18.51	34.8	36.99	52.48
0.3	17.09	18.74	34.2	37.43	51.87
0.4	16.75	18.93	33.6	37.82	50.82
0.5	16.39	19.09	32.9	38.16	49.92
0.6	16.02	19.2	32.2	38.42	48.95
0.7	15.63	19.27	31.5	38.58	47.9
0.8	15.21	19.25	30.6	38.59	46.72
0.9	14.74	19.12	29.7	38.33	45.3
1	13.96	18.42	28.1	36.77	42.65

Switching Angles (α_6-α_9)			
MI	**α_6**	**α_7**	**α_8**	**α_9**
0.1	54.71	71.13	72.95	89.1
0.2	55.39	70.24	73.68	88.19
0.3	56.04	69.33	74.57	87.28
0.4	56.64	68.37	75.28	86.36
0.5	57.18	67.27	76.05	85.41
0.6	57.69	66.3	76.79	84.42
0.7	58	65.11	77.47	83.37
0.8	58.14	63.73	78.04	82.06
0.9	57.82	61.92	78.23	80.61
1	54.93	57.71	73.47	73.47

TABLE IV. INDIVIDUAL ODD HARMONICS AND THD VALUES OBTAINED FROM PSO ALGORITHM.

MI	Selective harmonics						THD %
	H5	**H7**	**H11**	**H13**	**H17**	**H19**	
0.1	3.47	0.57	3.32	0.5	13.49	52.10	212.1
0.2	1.87	0.64	0.15	0.61	4.34	44.79	165.8
0.3	24.62	9.74	2.87	9.19	35.99	26.31	114.8
0.4	13.25	8.54	2.43	5.37	36.13	18.94	91.13
0.5	5.78	2.04	2.46	1.79	21.52	17.46	64.22
0.6	11.77	4.74	3.44	3.02	2.70	2.99	25.36
0.7	8.34	3.32	1.39	1.52	1.59	1.78	14.79
0.8	5.24	1.91	1.20	1.35	1.37	1.26	8.81
0.9	4.26	1.54	0.94	1.11	1.17	1.15	5.86
1	2.89	1.52	0.37	0.52	0.62	1.08	3.96

A. FFT Analysis of the Nonlinear Load

The Fast Fourier transform (FFT) spectrum of the voltage output and current output of the nine-switch inverter NSI_1 and NSI_2, respectively, at a V_{dc} of 24 V, is depicted in Figs. 7 and 8. The required switching angles are calculated offline using the PSO method, according to the purpose of the desired fundamental quantity. The obtained results are stored in Look-Up Tables (LUT). This execution approach is straightforward and does not require the usage of data acquisition cards. However, the magnitude of the LUT is directly correlated with the precision of the approach. The count of potential operational points can be evaluated employing extended LUTs. Sets of switching angles obtained from the PSO algorithm exhibit greater precision and a relatively rapid convergence rate. The effective control of the functioning of a nine-switch inverter fed nonlinear load is

achieved by utilising the appropriate value of the switching angle, which is acquired by PSO. The desired magnitude of the essential voltage at output is achieved by eliminating all the harmonics chosen.
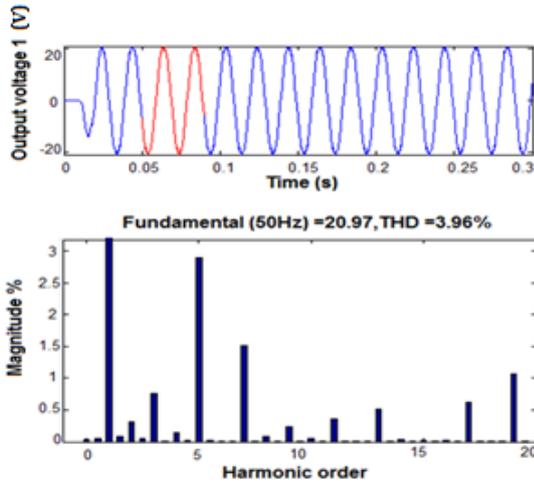
Fig. 7. FFT spectrum of the output voltage of SHEPWM control of nonlinear load$_1$.
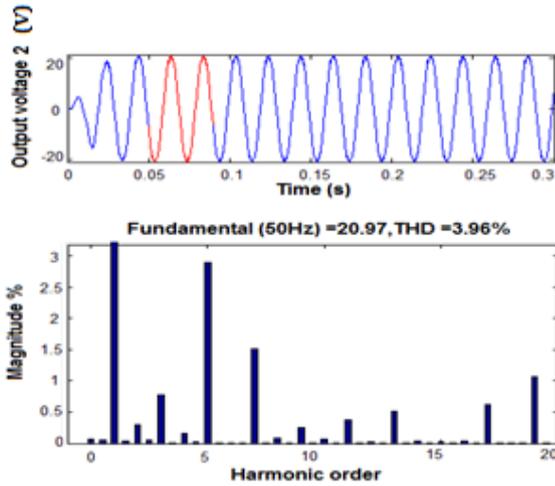
Fig. 8. FFT spectrum of output voltage of SHEPWM control of nonlinear load$_2$.

B. Experiment Results

The hardware prototype of the nine-switch inverter is subjected to testing using the PSO-based SHEPWM technique to verify the precision of the theoretical and simulation results. The NSI hardware circuit is used to generate the gating pulse for the PSO-based SHEPWM method, utilising the ATmega162 microcontroller. The switching angles derived from PSO were tuned for modulation indexes ranging from 0.1 to 1. An experimental prototype using an ATmega162 microcontroller is implemented with a voltage of Vdc = 24 V. The results of this implementation are studied using a Fluke 1735 power logger, as depicted in Fig. 9.

Fig. 9. Experimental setup of nine-switch inverter.

The IRF340 MOSFET, a power electronics device, is employed in NSI as a switching component. The DC link voltage is sustained at 24 V, and a diode bridge rectifier with a resistive load of 50 Ω is used as a nonlinear load is utilised. The particle swarm optimisation technique is used to generate the optimised firing angles for the switches. These angles are then inputted into the ATmega 162 microcontroller, where they are converted into pulses by turning the switches on and off in a specific sequence. The pulse width is then modulated, and the modified pulse is sent to the switches. Therefore, when switches are activated at those certain firing angles, the intended harmonics are effectively eliminated. Figure 10 shows the output voltage of the hardware nine-switch inverter V$_{rms}$ of 21.9 V and THD of 3.9 %.

(a)   (b)
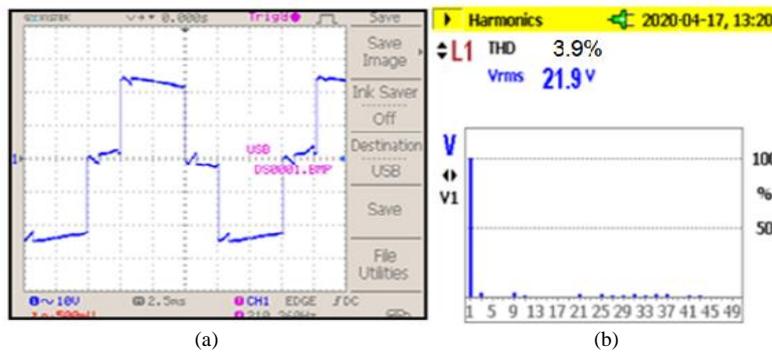
Fig. 10. Experimental outputs for nine-switch inverter: (a) Output voltage; (b) FFT spectrum for SHEPWM at MI = 1.

V. CONCLUSIONS

This work investigates the harmonic profile of a nine-switch inverter (NSI) control for both linear and nonlinear loads using the fundamental frequency selective harmonic elimination pulse width modulation (SHEPWM) switching approach. The output of the inverter powers both linear loads, such as two induction motors with varying speeds, and nonlinear loads [19], [20]. The performance of the NSI is

simulated using MATLAB-SIMULINK software, and the fast Fourier transform (FFT) spectrum is acquired. The utilisation of the high-frequency carrier with a PWM control in the nine-switch inverter results in reduced total harmonic distortion (THD) for linear load-1 and linear load-2. The THD values for the output voltages are 4.74 % and 4.71 %, respectively. However, the nonlinear load offers the output voltages have a higher THD value of 15.85 % when the 5th, 7th, 11th, 13th, 17th, and 19th harmonics are more prominent. The particle swarm optimisation (PSO)-based SHEPWM approach is employed to minimise the THD in a nonlinear load fed by NSI. The optimal switching angles are obtained by using the PSO technique. The PSO method provided a global minimum solution with rapid convergence. The achievement of the SHEPWM technique is compared to that of the CBPWM technique, and the solution sets are assessed based on the amplitude of the specific harmonics being targeted and the THD. The SHEPWM technique successfully removed the 5th, 7th, 11th, 13th, 17th, and 19th lower-order harmonics, resulting in a minimised THD value of 3.96 %. The hardware prototype is constructed using the ATmega 162controller, and empirical findings demonstrate a strong correlation with the simulation results.

ACKNOWLEDGMENT

CONFLICTS OF INTEREST

The authors declare that they have no conflicts of interest.

REFERENCES

[1] D. N. Zmood, D. G. Holmes, and G. H. Bode, "Frequency-domain analysis of three-phase linear current regulators", *IEEE Transactions on Industry Applications*, vol. 37, no. 2, pp. 601–610, 2001. DOI: 10.1109/28.913727.

[2] E. Ledezma, B. McGrath, A. Munoz, and T. A. Lipo, "Dual AC-drive system with a reduced switch count", *IEEE Transactions on Industrial Applications*, vol. 37, no. 5, pp. 1325–1333, 2001. DOI: 10.1109/28.952508.

[3] L. Zhang, P. C. Loh, and F. Gao, "An integrated nine-switch power conditioner for power quality enhancement and voltage sag mitigation", *IEEE Transactions on Power Electronics*, vol. 27, no. 3, pp. 1177–1190, 2012. DOI: 10.1109/TPEL.2011.2115256.

[4] F. Gao, L. Zhang, D. Li, P. C. Loh, Y. Tang, and H. Gao, "Optimal pulse width modulation of nine-switch converter", *IEEE Transactions on Power Electronics*, vol. 25, no. 9, pp. 2331–2343, 2010. DOI: 10.1109/TPEL.2010.2047733.

[5] M. Nirmala and S. Rameshselvakumar, "Nine switch converter based solar hybrid electric vehicle", *Pakistan Journal of Biotechnology*, vol. 14, special issue no. II, pp. 59–63, 2017.

[6] T. Kominami and Y. Fujimoto, "A novel nine-switch inverter for independent control of two three-phase loads", in *Proc. of 2007 IEEE Industry Applications Annual Meeting*, 2007, pp. 2346–2350. DOI: 10.1109/07IAS.2007.354.

[7] K. Baskaran and M. Nirmala, "Intelligent control based FRT capability of nine switch grid side converter fed DFIG system", *Journal of Electrical Engineering*, vol. 17, no. 3, 2017.

[8] P. C. Krause, O. Wasynczuk, and S. D. Sudhoff, *Analysis of Electric Machinery and Drive Systems*, 2nd ed., Wiley-IEEE Press, 2002. DOI: 10.1109/9780470544167.

[9] R. Kumar, R. A. Gupta, S. V. Bhangale, and H. Gothwal, "Artificial neural network based direct Torque Control of Induction Motor drives", in *Proc. of 2007 IET-UK International Conference on Information and Communication Technology in Electrical Sciences (ICTES 2007)*, 2007, pp. 361–367. DOI: 10.1049/ic:20070638.

[10] C. Liu, B. Wu, N. R. Zargari, D. Xu, and J. Wang, "A novel three-phase three-leg AC/AC converter using nine IGBTs", *IEEE Transactions on Power Electronics*, vol. 24, no. 5, pp. 1151–1160, 2009. DOI: 10.1109/TPEL.2008.2004038.

[11] F. Kong, J. Xia, D. Yang, and T. Lan, "Hydro-Turbine Coordination Power Predictive Method of Improved Multi-Layer Neural Network Considered Adaptive Anti-Normalisation Strategy", *Elektron Elektrotech*, vol. 29, no. 1, pp. 40-48, 2023. DOI: 10.5755/j02.eie.28599.

[12] G. Wen, Y. Chen, Z. Zhong, and Y. Kang, "Nine-switch-converter-based DFIG wind power system and its dynamic DC voltage assigned approach for low voltage riding through (LVRT)", in *Proc. of 2014 IEEE Energy Conversion Congress and Exposition (ECCE)*, 2014, pp. 4599–4605. DOI: 10.1109/ECCE.2014.6954030.

[13] L. M. Tolbert, J. Chiasson, K. McKenzie, and Z. Du, "Elimination of harmonics in a multilevel converter with nonequal DC sources", in *Proc. of Eighteenth Annual IEEE Applied Power Electronics Conference and Exposition*, 2003, pp. 589–595, vol. 1. DOI: 10.1109/APEC.2003.1179272.

[14] T. G. Kolda, R. M. Lewis, and V. Torczon, "Optimization by direct search: New perspectives on some classical and modern methods", *SIAM Review*, vol. 45, no. 3, pp. 385–482, 2003. DOI: 10.1137/S003614450242889.

[15] J. Kennedy and R. Eberhart, "Particle swarm optimization", in *Proc. of ICNN'95 - International Conference on Neural Networks*, 1995, pp. 1942–1948, vol. 4. DOI: 10.1109/ICNN.1995.488968.

[16] M. Nirmala, K. Baskaran, and S. Sowmiya, "Modified SVPWM fed nine switch inverter for motor load", *Pakistan Journal of Biotechnology*, vol. 14, special issue no. II, pp. 55–59, 2017.

[17] S. M. D. Dehnavi, M. Mohamadian, A. Yazdian, and F. Ashrafzadeh, "Space vectors modulation for nine-switch converters", *IEEE Trans. Power Electron.*, vol. 25, no. 6, pp. 1488–1496, 2010. DOI: 10.1109/TPEL.2009.2037001.

[18] A. Abdelhakim, P. Mattavelli, and G. Spiazzi, "Three-phase split-source inverter (SSI): Analysis and modulation", *IEEE Transactions on Power Electronics*, vol. 31, no. 11, pp. 7451–7461, 2016. DOI: 10.1109/TPEL.2015.2513204.

[19] A. Abdelhakim, P. Mattavelli, V. Boscaino, and G. Lullo, "Decoupled control scheme of grid-connected split-source inverters", *IEEE Transactions on Industrial Electronics*, vol. 64, no. 8, pp. 6202–6211, 2017. DOI: 10.1109/TIE.2017.2677343.

[20] J. Ebrahimi, E. Babaei, and G. B. Gharehpetian, "A new multilevel converter topology with reduced number of power electronic components", *IEEE Trans. Ind. Electron.*, vol. 59, no. 2, pp. 655–667, 2012. DOI: 10.1109/TIE.2011.2151813.